European Journal of Pharmacology 856 (2019) 172409

Contents lists available at ScienceDirect

European Journal of Pharmacology

journal homepage: www.elsevier.com/locate/ejphar

Full length article

Synergistic effects of gefitinib and thalidomide treatment on EGFR-TKI-sensitive and -resistant NSCLC

Xiaohong Xia[a,1], Yuan Liu[a,1], Yuning Liao[a,1], Zhiqiang Guo[a], Chuyi Huang[a], Fangcheng Zhang[b], Lili Jiang[a], Xuejun Wang[c], Jinbao Liu[a,**], Hongbiao Huang[a,*]

[a] Affiliated Cancer Hospital and Institute of Guangzhou Medical University, Key Laboratory of Protein Modification and Degradation, State Key Laboratory of Respiratory Disease, School of Basic Medical Sciences, Guangzhou Medical University, Guangzhou, Guangdong, 510095, China
[b] Guangzhou Institute of Cardiovascular Disease, The Second Affiliated Hospital, Guangzhou Medical University, Guangzhou, Guangdong, 510260, China
[c] Division of Basic Biomedical Sciences, Sanford School of Medicine of the University of South Dakota, Vermillion, SD, 57069, USA

ARTICLE INFO

Keywords:
Lung cancer
Thalidomide
Gefitinib
EGFR-TKI resistant
p-EGFR

ABSTRACT

EGF receptor tyrosine kinase inhibitors (EGFR-TKIs) have been widely used as a standard therapy in non-small cell lung cancer (NSCLC) patients with EGFR mutations. However, most if not all of the patients who initially have responded to EGFR-TKIs later experience progression or deterioration of the disease while still on the treatment. Drug resistance becomes inevitable due to the emergence of the second-site EGFR T790M mutation within exon 20, MET and HER2 amplification, small cell histologic transformation and rare secondary BRAF mutations. The acquired drug resistance limits the efficacy of EGFR-TKIs in patients. Thalidomide is a widely used anti-angiogenic and immunomodulatory drug with anticancer effects. The current study was aimed to explore the combined effects of gefitinib and thalidomide on NSCLC. The combination of thalidomide and gefitinib induced antiproliferative and proapoptotic effects in HCC827, PC9, and PC9GR cells. The inhibition of EGFR phosphorylation and downstream signaling was more pronounced in the thalidomide and gefitinib co-treatment group as compared with the single agent treatment groups. Further study revealed that the inhibitors of AKT, MEK/ERK, and p38 increased the antiproliferative and proapoptotic effects of the combined treatment of thalidomide and gefitinib. However, JNK inhibition moderately abrogated cell apoptosis induced by the co-treatment. In conclusion, thalidomide and gefitinib exhibit synergistic effects on both TKI-sensitive and -resistant NSCLC cells by targeting the EGFR signaling pathways, suggesting that the combination strategy is promising for the treatment of NSCLC.

1. Introduction

Lung cancer is a common malignancy and the leading cause of cancer-related deaths worldwide. Moreover, non-small-cell lung cancer (NSCLC) accounts for approximately 85% of lung cancers (Bray et al., 2018; Chen et al., 2014; Silvestri and Spiro, 2006). Initially, chemotherapeutic agents such as cisplatin and docetaxel were applied to most NSCLC patients; however, the patients did not respond to these treatments due to drug resistance (Fan et al., 2014). The epidermal growth factor receptor (EGFR) plays a critical role in the growth and progression of a large proportion of human cancers, especially NSCLC (Loong et al., 2018; Mitsudomi and Yatabe, 2010). EGFR is overexpressed in approximately 40–80% of NSCLC cases and its overexpression predicts poor survival and prognosis (Raymond et al., 2000; Wang et al., 2018; Yochum et al., 2019). Gefitinib, a small-molecule EGFR tyrosine kinase inhibitor (TKI), has shown impressive therapeutic effects on the NSCLC patients with EGFR mutations, and thus, is recognized as the standard first-line therapy (Nguyen and Neal, 2012; Soria et al., 2012). Additionally, a point mutation in exon 20 of EGFR causing a threonine-to-methionine substitution at amino acid position 790 (T790M) was authenticated in patients who developed drug resistance within 9–15 months after treatment with TKIs (Pao et al., 2005; Shih et al., 2005). About 60% of the patients who have acquired resistance to EGFR-TKIs harbor the T790M mutation (Kosaka et al., 2006; Sequist et al., 2011; Yu et al., 2013). Hence, novel therapeutics to overcome or reduce the drug resistance are urgently needed

* Corresponding author.
** Corresponding author.
E-mail addresses: jliu@gzhmu.edu.cn (J. Liu), huanghongbiao@gzhmu.edu.cn (H. Huang).
[1] Equal contribution.

https://doi.org/10.1016/j.ejphar.2019.172409
Received 11 March 2019; Received in revised form 19 May 2019; Accepted 22 May 2019
Available online 25 May 2019

by patients with NSCLC.

Thalidomide is a derivative of glutamic acid that was used initially as a nonbarbiturate sedative-hypnotic in clinics in the late 1950s (Kumar et al., 2002; Lenardo and Calabrese, 2000). In 1998, the United States Food and Drug Administration (FDA) approved thalidomide for its striking effect on patients with erythema nodosum leprosum (ENL). In addition, it improves the treatment of aphthous ulcers, HIV-wasting syndrome, and chronic graft-versus-host disease. Owing to the anti-angiogenic and immunomodulatory actions of thalidomide, it has been extensively applied as a therapeutic to multiple myeloma (MM) (Bartlett et al., 2004; Kumar and Rajkumar, 2005). Lenalidomide and pomalidomide, analogs of thalidomide, have been approved by the FDA for the treatment of MM based on the satisfactory outcome in clinical trials (Andhavarapu and Roy, 2013; Chanan-Khan et al., 2013; Gras, 2013). Thalidomide has also been found to be effective on some solid tumors, including hepatocellular cancer and NSCLC (Pinter et al., 2008; Woo et al., 2016). Also, it inhibits the metastasis of solid carcinoma cells (Lin et al., 2006).

Herein, we sought to determine the combined effect of thalidomide and gefitinib on the growth, proliferation, and progression of NSCLC cells. Thus, several EGFR-TKIs-sensitive human NSCLC cell lines and one with resistance to gefitinib have been selected. The combination strategies displayed a marked therapeutic effect on both the TKI-sensitive and the TKI-resistant NSCLC cells. Overall, the present study provides a promising combination strategy for patients with NSCLC, especially those with EGFR mutations.

2. Materials and methods

2.1. Materials

Gefitinib (S1025), thalidomide (S1193), SB203580 (S1076), SP600125 (S1460), MK2206 (S1078), and PD0325901 (S1036) were obtained from Selleckchem (Houston, TX, USA), solubilized in DMSO, and stored at −20 °C. MTS (G111) was obtained from Promega (Madison, WI, USA). The following antibodies were procured from Cell Signaling Technology (MA, USA): anti-PARP (9542s), anti-cleaved caspase 3 (9661s), anti-cleaved caspase 9 (9501s), anti-Bcl-2 (15071s), anti-Bcl-XL (2764), anti-Bax (5023s), anti-CDK4 (12790s), anti-CDK2 (2546p), anti-cyclinD1(29269), anti-cleaved caspase 8 (9496s), anti-phospho-EGFR (Y1173) (4407s), anti-EGFR (4267s), anti-total-MEK (9126), anti-phospho-MEK (Ser217/221) (9154), anti-total-ERK (4695p), anti-phospho-ERK (Thr202/Tyr204) (4370s), anti-total-p38 (8690p), anti-phospho-p38 (Thr180/Tyr182) (4511s), anti-total-JNK (9252s), anti-phospho-JNK (Thr183/Tyr185) (9255s), anti-total-AKT (9272), anti-phospho-AKT (Ser473) (4060s), and anti-GAPDH (14C10). For Western blot analyses, the above antibodies were used at 1:1000. For immunofluorescence assay, the dilutions were as follows: p-EGFR (1:800), p-AKT (1:400), and p-ERK (1:200). For immunohistochemical staining assays, the dilution of p-EGFR and of Ki67 were 1:400. Annexin V-FITC/PI apoptosis detection kits (KGA107) were purchased from Keygen Company (Nanjing, China). Cell Lysis Buffer (9803) was obtained from Cell Signaling Technology and maintained at −20 °C. Rhodamine123 (CT0047) was purchased from Leagene Biotechnology Company (Beijing, China).

2.2. Cell lines and culture conditions

The human NSCLC cell lines, including HCC827, A549 and H1299 were purchased from American Type Culture Collection (ATCC; Manassas, VA, USA). Gefitinib sensitive PC9 cells and gefitinib-resistant PC9GR cells were gifted by Dr. M. Liu from Guangzhou Medical University (China).The cells were cultured in 75 cm cell culture flasks containing 20 ml of RPMI 1640 medium with 10% fetal bovine serum (FBS) at 37 °C and 5% CO_2.

2.3. Cell viability assay

As reported previously, the inhibition of growth was assessed with the MTS assay (Huang et al., 2011; Xia et al., 2018). HCC827, PC9, PC9GR, A549, and H1299 cells were trypsinized, collected, suspended in RPMI 1640 medium with 10% FBS, and plated at a density of 2500 cells in 100 µl in 96-well plates. The cells were treated with gefitinib, thalidomide, or the combination of both drugs for a specified period after incubation for 48 h. A volume of 20 µl MTS reagent was added to each well and the mixture was incubated for additional 3 h. The optical density was measured on a microplate reader at 490 nm.

2.4. Colony formation assay

According to the previously established methods (Cai et al., 2017; Liao et al., 2018), HCC827, PC9, and PC9GR cells exposed to z-VAD-FMK, thalidomide and gefitinib (T + G), or the combination of the three drugs for 24 h were trypsinized, suspended in 6-well plates containing 30% agarose supplemented with 10% FBS in RPMI-1640 medium, and cultured at 37 °C and 5% CO_2. After 10 days, the cells were fixed with 4% paraformaldehyde for 15 min, followed by phosphate-buffered saline (PBS) washes and stained with 1% crystal violet solution. The images were visualized using a digital camera.

2.5. EdU staining

The cell proliferation was detected using Cell-Light™ EdU Apollo 567 In Vitro Kit (Cat. number: C10310-1, RiboBio, Guangzhou, China). PC9 and PC9GR cells were plated onto chamber-slides and treated with thalidomide or gefitinib or co-treatment for 24 h. Subsequently, the cells were incubated with 50 µmol/L EdU for 2 h at 37 °C and fixed with 4% paraformaldehyde, followed by quenching with 2 mg/ml glycine and washing with PBS for 5 min. Then, the cells were permeabilized with 0.5% Triton X-100 for 10 min and washed with chilled PBS. The Apollo reaction cocktail containing annexing agent buffer, fluorochrome, a catalytic agent, and Apollo reaction buffer were added to the cells and washed with 0.5% Triton X-100 after 30 min. Subsequently, the Fluoroshield mounting medium with DAPI (Abcam) was added for DNA staining in the dark. Images were captured using a fluorescence microscope.

2.6. Cell death assay

Apoptosis was determined by flow cytometry as described previously (Huang et al., 2010; Liao et al., 2017). 1×10^5 HCC827, PC9, or PC9GR cells/well were plated in 6-well plates and treated with either gefitinib, thalidomide, or the combination of both for 24 h. A cohort of the treated cells was digested and harvested. Then, the cells were washed with chilled PBS, suspended with 500 µl binding buffer, and detected by flow cytometry after staining with Annexin V-FITC/PI in the dark.

2.7. Western blot

The assay was performed as described previously (Huang et al., 2017a). HCC827, PC9, and PC9GR cells were exposed to the same drugs, and total proteins were extracted using cell lysis buffer with protease inhibitors, phosphatase inhibitors, and PMSF (Keygen, Nanjing, China). The BCA protein assay kit was used to determine the protein concentration. An equivalent amount of protein samples was subject to SDS-PAGE and transferred to PVDF membranes. Then, the membranes were blocked with 5% defatted milk powder in PBS-T for 1 h and washed three times. Subsequently, the membrane was probed with primary antibodies overnight, followed by incubation with appropriate secondary antibodies for 1 h. Finally, the ECL detection reagents were used for the detection of immunoreactive bands and

exposed to X-ray films (Kodak, Japan).

2.8. Immunofluorescence assay

Immunofluorescence assay was performed as described previously (Cai et al., 2017). Briefly, the cells treated with thalidomide and/or gefitinib were fixed with 4% paraformaldehyde. Then, the cells were washed with PBS three times, followed by permeabilization with 0.1% Triton X-100 (Solarbio Life Science). After 10 min, the cells were blocked with 5% BSA for 30 min and probed with primary antibodies in 1% BSA overnight at 4 °C. Then, the cells were incubated with secondary Cy3-conjugated antibody. Subsequently, DAPI with fluoroshield mounting medium was added, and images captured using a fluorescence microscope.

2.9. Mitochondrial membrane integrity measurement

As we previously reported, the mitochondrial membrane potential was detected using Rhodamine-123 (Huang et al., 2017b). The cells were exposed to thalidomide, gefitinib, or the combination of both for 18 h. The treated cells were harvested and washed with PBS, followed by staining with 1 μM of Rhodamine-123 for 20 min at 37 °C. Flow cytometry was used to determine the mitochondrial membrane potential.

2.10. Nude mouse xenograft model

The nude mice were obtained from the Guangzhou University of Chinese Medicine. The animal protocols were approved by the Institutional Animal Care and Use Committee of Guangzhou Medical University. The nude BALB/c female mice (18–22 g) were housed in the quarantine room for inspection for 2–3 days. Then, the mice were transferred to the animal barrier facilities of Guangzhou Medical University. Food and water were supplied adequately. Approximately 5×10^6 PC9 cells were implanted subcutaneously on the flanks of each mouse for 10 days. The animals were divided randomly into 4 groups and orally administered thalidomide (30 mg/kg/2 d) and/or gefitinib (7.5 mg/kg/2 d) for 2 weeks. Tumor volumes and mouse body weights were measured on every alternate day.

2.11. Immunohistochemical staining

This assay was performed as described previously (Huang et al., 2016). Briefly, the formalin-fixed and paraffin-embedded tumor tissues were sectioned and immunostained for p-EGFR and Ki67 using the MaxVision Kit (Maixin Biol). The fluorescent-labeled secondary antibodies were detected with DAB.

2.12. TUNEL assay

The sections of the tissues were steeped with xylene and 100% ethanol, followed by ethanol (90%, 80%, 70%) and PBS washes. Then, the samples were incubated with proteinase K at 20 μg/mL for 20 min. After PBS washes, the samples were incubated with DNase I buffer for 10 min and washed again with ddH_2O three times. Lastly, the samples were incubated with equilibration buffer, Alexa Fluor 488-12-dUTP labeling mix, and recombinant TdT Enzyme. TUNEL-positive cells (green) were detected with a fluorescence microscope; DAPI stained the nucleus blue.

2.13. Combination index

The interaction between the two agents drugs was determined by counting the combination index (CI). The Chou-Talalay equation for classic isobologram was used to calculated the CI (Chou and Talalay, 1984). The general equation is as follows: CI = (D) 1/(Dx) 1 + (D) 2/(Dx) 2. (D) 1 and (D) 2 respectively indicate the concentrations of compounds 1 and 2, inducing an combinational effect. Dx is the dose of one drug alone necessary to produce the same effect. CI > 1 indicates antagonism. CI = 1 shows additivity. CI < 1 defines synergy.

2.14. Statistical analysis

The quantitative data of all experiments are presented as mean ± standard deviation (S.D.) from three independent experiments. Unpaired Student's t-test or one-way ANOVA was applied to determine the statistical probabilities. GraphPad Prism 5.0 software was used for all the statistical analyses. P value < 0.05 is considered statistically significant.

3. Results

3.1. Effect of thalidomide and gefitinib combination on the growth and proliferation of NSCLC

To evaluate the effects of thalidomide at different doses combined with gefitinib on the cell proliferation of NSCLC, we performed MTS assays on several NSCLC cell lines. Since the drug resistance is a major issue, we also examined the effect of the co-treatment on the gefitinib-resistant PC9GR cells. The cell viability of NSCLC cells was inhibited with the increasing doses of gefitinib. However, the effects of anti-proliferation were more obvious on PC9 and HCC827 cells carrying the EGFR-mutation than on the wild-type A549 and H1299 cells (Fig. 1A). Next, we found that the proliferative activity of PC9GR was not suppressed considerably until the dose was raised to 10 μM, suggesting that PC9GR harbors additional mutations, which results in low sensitivity to EGFR-TKI (Fig. 1A). Then, we assessed the antiproliferative effects of a combination of thalidomide with gefitinib. As shown by the MTS analysis (Fig. 1A), a panel of NSCLC cells displayed enhanced sensitivity to gefitinib after exposure to thalidomide. Furthermore, the proliferation of the cells was synergistically inhibited by an increased concentration of thalidomide for 48 h. In addition, the CI values were calculated as a quantitative measure of the degree of interaction between different drugs. As shown in Fig. 1B and Fig. S1, CI values were < 1, suggesting that thalidomide and gefitinib resulted in synergistic growth inhibition in HCC827, PC9, PC9GR, A549, and H1299 cells (Fig. 1B; Fig. S1). The results confirmed a robust growth inhibition by adding thalidomide to gefitinib in HCC827, PC9, PC9GR, A549, and H1299 cell lines. Moreover, EdU staining showed that PC9 and PC9GR cells co-treated with thalidomide and gefitinib had less proliferative capacity than cells treated with thalidomide or gefitinib alone (Fig. 1C). These results indicated that thalidomide sensitizes lung cancer cells to gefitinib and enhances the inhibition of gefitinib-induced proliferation.

3.2. Effect of thalidomide and gefitinib combination on cell cycle progression and cell migration/invasion in NSCLC cell lines

The above findings showed that the co-treatment of thalidomide and gefitinib induced greater growth suppression than each solo treatment. To further clarify the mechanism underlying the efficiency of the combination of gefitinib and thalidomide than the single treatment, we used flow cytometry to detect the cell cycle progression in each group exposed to thalidomide or gefitinib or the combination of thalidomide and gefitinib. The result demonstrated that gefitinib dramatically arrested the cell cycle at G0/G1 phase without significant differences in cycle progression between gefitinib and the combined treatment group (Figs. S2A and B). Western blot results showed that the levels of CDK4, CDK2, and cyclin D1, which are key proteins promoting G1 to S transition, were downregulated by gefitinib. However, this downregulation was not enhanced by thalidomide (Fig. S2C). Taken together, thalidomide does not enhance the cell cycle arrest induced by gefitinib. Moreover, we detected the ability of cell migration and invasion of NSCLC cells exposed to the co-treatment. Results from wound

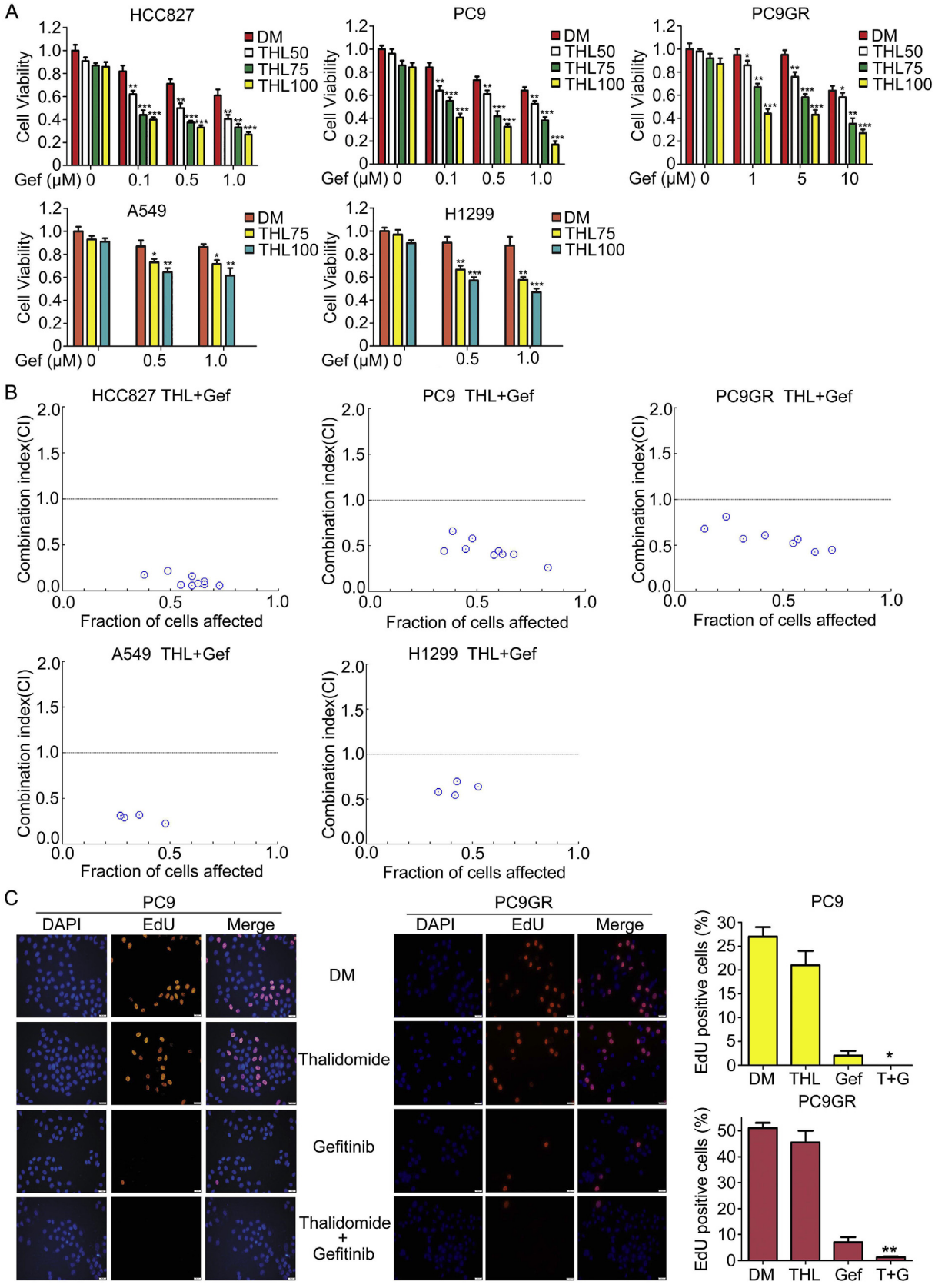

Fig. 1. Effect of thalidomide and gefitinib in combination on NSCLC growth and proliferation. (**A**) Cells were exposed to thalidomide (THL), gefitinib (Gef), and THL + Gef (T + G). Cell viability was assessed using MTS assay after treatment for 48 h. Data were obtained from three independent experiments. *P < 0.05, **P < 0.01, ***P < 0.001 *vs.* each treatment alone. THL 50, THL75 and THL100 denote THL used at 50, 75, and 100 μM, respectively. (**B**) The interaction between thalidomide and gefitinib was evaluated by combination index (CI). (**C**) Cells were exposed to thalidomide (75 μM), gefitinib (0.1 μM for PC9, 10 μM for PC9GR), and the combination of both. Cell proliferation was measured with EdU staining. Cells were incubated with EdU for 2 h and processed for immunofluorescence staining. Nuclei were stained with DAPI. Three independent experiments were performed. The cell proliferation was quantitated, and representative images are shown. *P < 0.05, **P < 0.01 *vs.* each treatment alone. DM, DMSO.

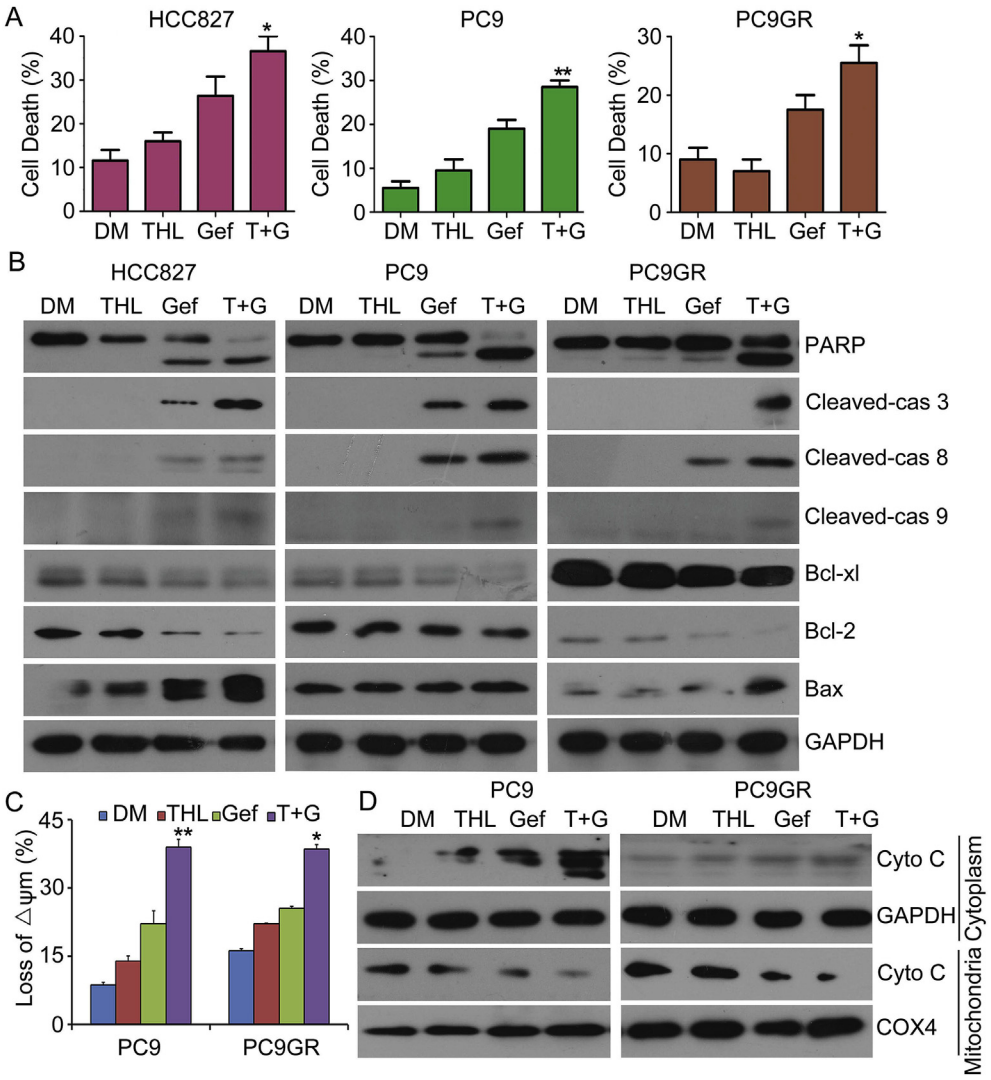

Fig. 2. Induction of apoptosis by the combined treatment of gefitinib and thalidomide in NSCLC cell lines. HCC827, PC9, and PC9GR cells were exposed to thalidomide (75 μM), gefitinib (0.1 μM for HCC827 and PC9, 10 μM for PC9GR), or the combination. The cells were stained with AnnexinV-FITC/PI, followed by detection with flow cytometry. (**A**) Quantification of cell death. *P < 0.05, **P < 0.01 *vs.* each treatment alone. (**B**) Total proteins were collected from the treated cancer cells, and Western blot analyses for the expression of cleaved caspase-3, -8, and -9, as well as PARP, Bcl-XL, Bcl-2, and Bax were performed. GAPDH was used as a loading control. (**C**) PC9 and PC9GR cells were exposed to thalidomide, gefitinib, or the combination of both (T + G). The cells were stained with rhodamine-123 and assessed by flow cytometry. The proportion of cells with loss of ΔΨ was shown. Three independent experiments were performed. Mean ± S.D. (n = 3). *P < 0.05, **P < 0.01 *vs.* each treatment alone. (**D**) Cytochrome C was analyzed with Western blots.

healing and transwell migration/invasion assays showed that the co-treatment of thalidomide and gefitinib more effectively inhibited NSCLC cell migration and invasion than gefitinib treatment alone (Figs. S3A–C).

3.3. Induction of apoptosis by the combined treatment of gefitinib and thalidomide in NSCLC cell lines

MTS assay showed that thalidomide and gefitinib significantly inhibited the growth of HCC827, PC9, and PC9GR cell lines. Thus, these were selected as experimental target cell lines. In order to further explore whether the increased growth inhibition induced by thalidomide in combination with gefitinib is due to induction of apoptosis, we analyzed the rates of apoptosis in lung cancer cells treated with gefitinib alone or with the combination of gefitinib and thalidomide for 24 h. The Annexin V-FITC/PI assay showed that cell apoptosis was markedly enhanced by the combined treatment as compared to the single treatment in HCC827 cells. Similar phenomena were also observed in PC9 and PC9GR cells (Fig. 2A).

Next, we examined the changes in the molecules vital for apoptosis. The proteolytic activity of caspase-3, -8, and -9 is regarded as apoptotic "executor" whereas PARP cleavage is induced by activated caspase-3, generating an 89-kDa apoptotic fragment (Matarrese et al., 2007). We found that the cleavage of PARP was induced by gefitinib in HCC827, PC9, and PC9GR cell lines; however, more abundant 89-kDa PARP apoptotic fragment was detected in the thalidomide and gefitinib combination groups. In addition, substantial cleavage of caspase-3, -8, and -9 was induced by the combination treatment as compared to the single agent treatment. The downregulation of the anti-apoptotic proteins Bcl-XL and Bcl-2 as well as the upregulation of the pro-apoptotic protein Bax were remarkably greater in the thalidomide and gefitinib co-treatment group than the single agent groups (Fig. 2B). These results indicate that thalidomide significantly enhances cell apoptosis induced by gefitinib in NSCLC cell lines.

Mitochondria play a major role in the regulation of apoptosis (Frenzel et al., 2009). Rhodamine-123 staining followed by flow cytometry revealed a low mitochondrial membrane potential (MMP) in the cells treated with the combination of thalidomide and gefitinib (Fig. 2C). The cytosolic and mitochondrial fractions were extracted in PC9 and PC9GR cell lines. The expression of cytochrome C was detected using Western blot analyses and the levels of cytoplasmic cytochrome C were found to be discernibly higher in the co-treatment group than in other groups (Fig. 2D). These findings indicated that thalidomide enhances the downregulation of MMP induced by gefitinib in NSCLC cell lines.

3.4. Induction of apoptosis by the co-treatment depends on caspase activation

As shown in Fig. 2, caspase pathways were activated by the

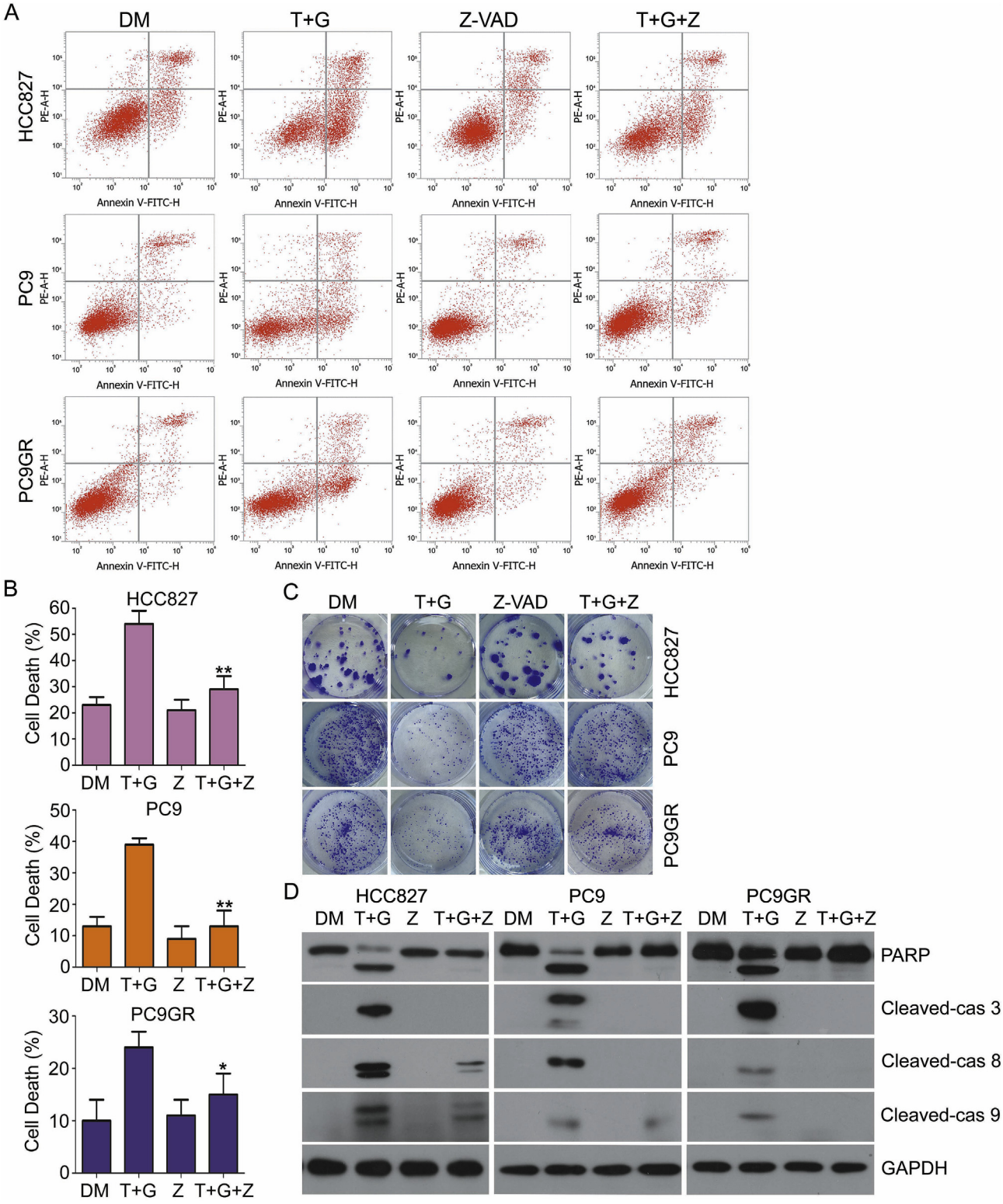

Fig. 3. Induction of apoptosis by the T + G co-treatment depends on caspases activation. HCC827, PC9, and PC9GR cells were exposed to the combination of thalidomide (75 μM) and gefitinib (0.1 μM for HCC827 and PC9, 10 μM for PC9GR) in the absence or presence of z-VAD-FMK (50 μM). Cells were harvested and stained with Annexin V-FITC/PI and assessed by flow cytometry for the detection of cell death. Representative images (**A**) and quantification of cell death (**B**) are shown. Data are represented as the mean ± S.D., n = 3. *P < 0.05, **P < 0.01 *vs.* T + G treatment group. The treated cells were transplanted in 30% agarose for 10 days after treatment for 24 h. (**C**) The images are selected from three independent experiments. (**D**) Representative images of Western blot analyses for changes in the expression of PARP and cleaved caspase-3, -8, and -9 induced by the indicated treatment.

treatment of thalidomide in combination with gefitinib. To further investigate this result, we tested the apoptotic rates following the z-VAD-FMK treatment in the combined treatment group using Annexin V-FITC/PI staining followed by flow cytometry. We found that the pan-caspase inhibitor z-VAD-FMK abrogated the apoptosis induced by the combination of thalidomide and gefitinib (Fig. 3A and B). Additionally, the colony-forming ability of NSCLC cells was detected. As shown in Fig. 3C, the number of colonies formed was increased by adding z-VAD-FMK. Subsequently, we assessed the expression of apoptosis-related proteins using Western blot analyses, which yielded the findings that the increased expressions of cleaved PARP, caspase-3, -8, and -9 by the combination treatment of thalidomide and gefitinib were abrogated by z-VAD-FMK (Fig. 3D). Taken together, these results consistently indicate that apoptosis induced by the combined treatment requires caspase activation.

3.5. Effect on intracellular signaling pathway by the combined treatment of thalidomide and gefitinib in NSCLC cell lines

EGFR tightly regulates the cell growth and angiogenesis in tumors (Jones and Rappoport, 2014). To further explore the mechanism by which the combined treatment of thalidomide and gefitinib (T + G) exerts pro-apoptosis and growth inhibition effects, we assessed the phosphorylation of EGFR. Western blot assays revealed that the expression of phosphorylated EGFR was decreased in both the gefitinib group and the combination group, with a more pronounced down-regulation in the combination group. EGFR phosphorylation activates the AKT/ERK pathway which in turn promotes cell proliferation and cell survival (Roberts and Der, 2007); hence, changes in these molecular pathways would provide important clues for the potential mechanism governing the effects of thalidomide and gefitinib. Therefore, we examined the phosphorylation status of AKT, MEK and ERK, a widely used indicator for the activities of the related pathways. We found that the phosphorylation of AKT, MEK and ERK were suppressed significantly after the treatment of T + G. Since the phosphorylation of p38 and JNK were increased after gefitinib treatment and associated with gefitinib-induced cytotoxicity in lung cancer cells (Ko et al., 2013; Lu et al., 2011), we examined whether thalidomide increased the gefitinib-induced phosphorylation of p38 and JNK. Western blot assay showed that the phosphorylation of these molecules were increased by gefitinib and the combined treatment with thalidomide enhanced this effect (Fig. 4A).

In order to decipher whether thalidomide, gefitinib, and T + G treatments yield differential effects on nuclear translocation of p-EGFR, p-ERK, and p-AKT, we used immunofluorescence microscopy to examine the subcellular distribution and expression of these proteins in PC9GR cells that had been exposed to thalidomide, gefitinib, or the combination of both for 12 h. We found that p-EGFR, p-ERK, and p-AKT were localized in both the nucleus and cytoplasm; the gefitinib treatment and the combined treatment differentially decreased the expression of p-EGFR, p-ERK, and p-AKT but neither treatment altered the proportional distribution of these proteins between the nucleus and cytoplasm (Fig. 4B); and moreover, the immunofluorescence intensity of p-EGFR, p-ERK, and p-AKT were lower in the combined treatment group than in other groups (Fig. 4C), which is consistent with the results from Western blot analyses described earlier.

3.6. Inhibition of MAPKs and PI3K/AKT signaling pathways induces apoptosis by the co-treatment with thalidomide and gefitinib

To investigate whether MAPK signaling pathways play a critical role in apoptosis induction by the combined treatment of thalidomide and gefitinib, we used the small molecule inhibitors of MEK/ERK and JNK and found that MEK/ERK inhibitor (PD0325901) enhanced the induction of apoptosis by T + G as revealed by flow cytometry (Fig. 5A). Western blot analysis showed that the expressions of cleaved caspase-3, -8, -9, and PARP were upregulated by MEK/ERK inhibition (Fig. 5C). Furthermore, the expressions of cleaved PARP, caspase-3, -8, and -9 induced by the treatment of thalidomide combined with gefitinib were suppressed, and the ratio of cell death was decreased by the addition of JNK inhibitors (SP600125) (Fig. 5B and D), indicating that JNK mediated the caspase activation as well as cell death by T + G combination treatment.

In addition, to further explore the mechanism underlying the thalidomide-mediated increase in gefitinib-induced apoptosis, we examined other downstream signaling pathways of EGFR phosphorylation using the inhibitors of AKT (MK2206) and of p38 (SB203580). The MTS assays showed that the inhibition of AKT or p38 phosphorylation increased the T + G-induced antiproliferation effect (Fig. 6A and D; Figs. S4A and D). Moreover, the number of apoptotic cells was increased by the combined treatment of thalidomide and gefitinib (Fig. 6B and E; Figs. S4B and E). The inhibition of AKT exacerbated the expressions of cleaved PARP and caspase-3 (Fig. 6F; Fig. S4F). Surprisingly, the inhibition of p38 accelerated the growth inhibition and apoptosis induction by the co-treatment, similarly to AKT inhibition; however, p38 inhibition did not mitigate the effects of the T + G treatment on the protein levels of cleaved PARP and caspase-3 (Fig. 6C; Fig. S4C). We speculate that p38 might not be intimately involved in the activation of the specific caspases by the combination treatment. These findings indicate that suppression of MAPKs and AKT signaling pathways are involved in the apoptosis induction by the thalidomide and gefitinib combined treatment.

3.7. Co-treatment of thalidomide and gefitinib suppressed the growth of NSCLC in vivo

Since our in vitro experiments have demonstrated that the combination of thalidomide and gefitinib synergistically inhibit the cell proliferation, induce apoptosis, and suppress PI3K/MAPK signal transduction, we assessed the effect of thalidomide and gefitinib on tumor growth in vivo. The PC9 cells were implanted subcutaneously into nude mice. The mice carrying xenografts were divided into the vehicle, the thalidomide, the gefitinib, and the combination of thalidomide and gefitinib treatment groups. The tumor weights and sizes were significantly suppressed in the combination group as compared to the treatment with gefitinib or thalidomide alone, while the body weights did not display a significant difference among the groups (Fig. 7A–D). Subsequently, immunochemical staining revealed that the levels of phosphorylated EGFR and Ki67 were decreased in xenograft tumor tissues treated by gefitinib; importantly, these changes were enhanced by adding thalidomide to the gefitinib treatment (Fig. 7E). We found that apoptosis was upregulated in the combination group as compared to the treatment of either drug alone as indicated by TUNEL assays (Fig. 7F and G).

4. Discussion

In recent years, the invention of thalidomide represents a critical advancement in the anti-angiogenesis strategy for anticancer therapies (Kirchmair et al., 2007; McMeekin et al., 2007; Son et al., 2006). Thus, thalidomide has been used as a therapy for solid tumors, including hepatocellular carcinoma and renal cell cancer in phase II trials (Chuah et al., 2007; Stein and Rivera, 2007). Importantly, to achieve the expected results in clinical studies, the dose of thalidomide, 200–800 mg/day, affects the differentiation of murine embryonic cells. Reportedly, thalidomide presented a meaningful curative effect at 100 mg/day in combination with some other chemotherapeutic drugs, which was safe for the patients (Qiao et al., 2015; Rajkumar et al., 2002). These combinations of thalidomide with other chemotherapeutics not only reduced the teratogenicity but also achieved a satisfactory therapeutic effect in patients (Arcila et al., 2011). Gefitinib has been used as a first-line treatment for lung cancer with EGFR mutations. Because of the

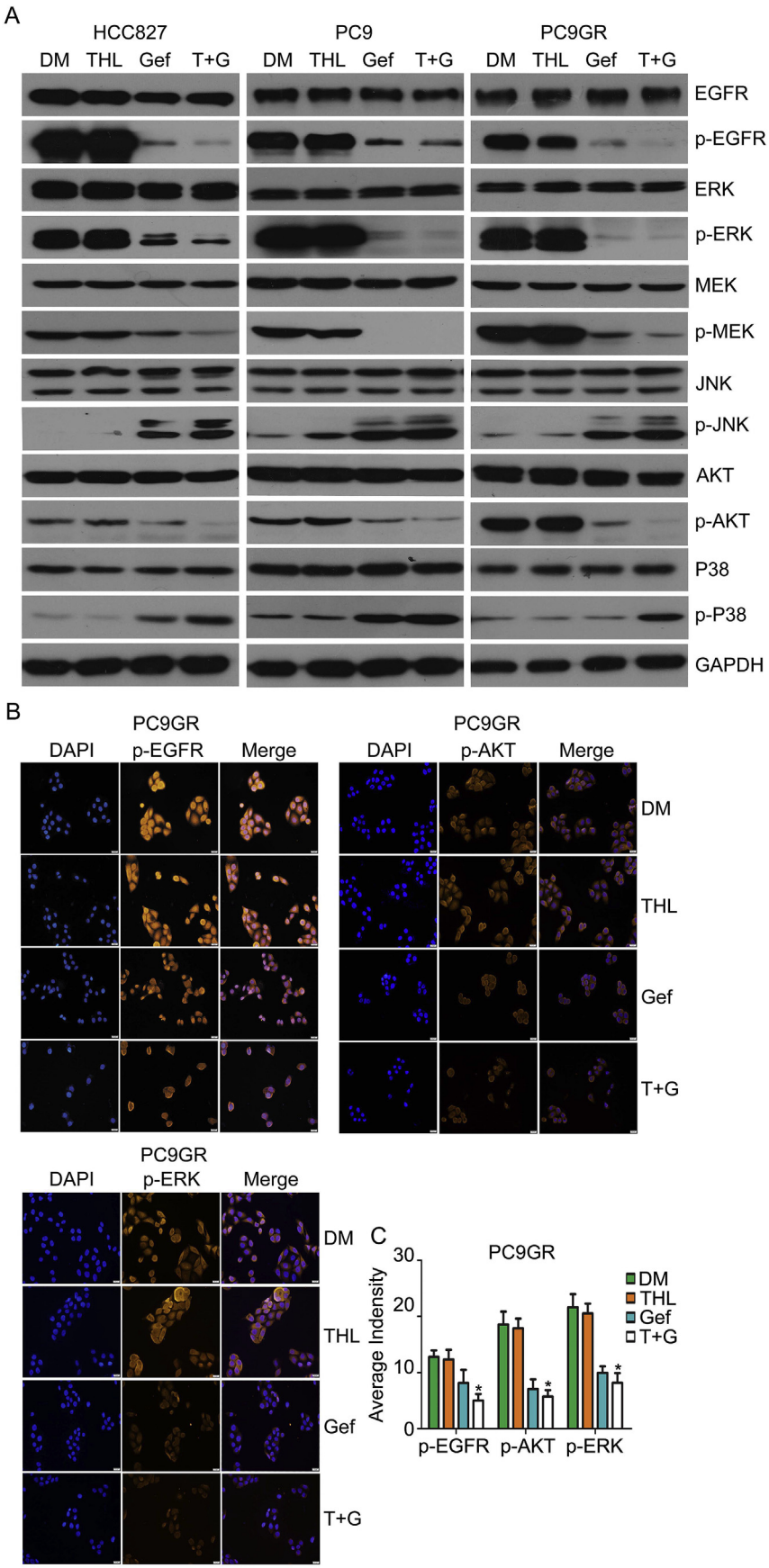

Fig. 4. Effect of the combined treatment of thalidomide and gefitinib on the intracellular signaling pathways in NSCLC cell lines. The lung cancer cells were treated with thalidomide (75 μM), gefitinib (0.1 μM for HCC827 and PC9, 10 μM for PC9GR), or the combination of the two drugs for 24 h. (**A**) Total proteins were collected from the treated cells. EGFR, AKT, MEK, ERK, JNK, and p38 activation were examined using Western blot analysis for specific phosphorylation. (**B**) The lung cancer cells were incubated for 12 h with thalidomide, gefitinib, or both drugs. The treated cells were incubated with the primary antibody at 4 °C overnight, followed by incubation with secondary Cy3-conjugated antibodies for 1 h. The nucleus was stained with DAPI. The micrographs of p-EGFR, p-AKT, and p-ERK immunofluorescence as well as the nuclear staining were recorded via a fluorescence microscope. (**C**) Fluorescence intensity was quantitated. Data are presented as the mean ± S.D., n = 3. *P < 0.05 *vs*. each treatment alone.

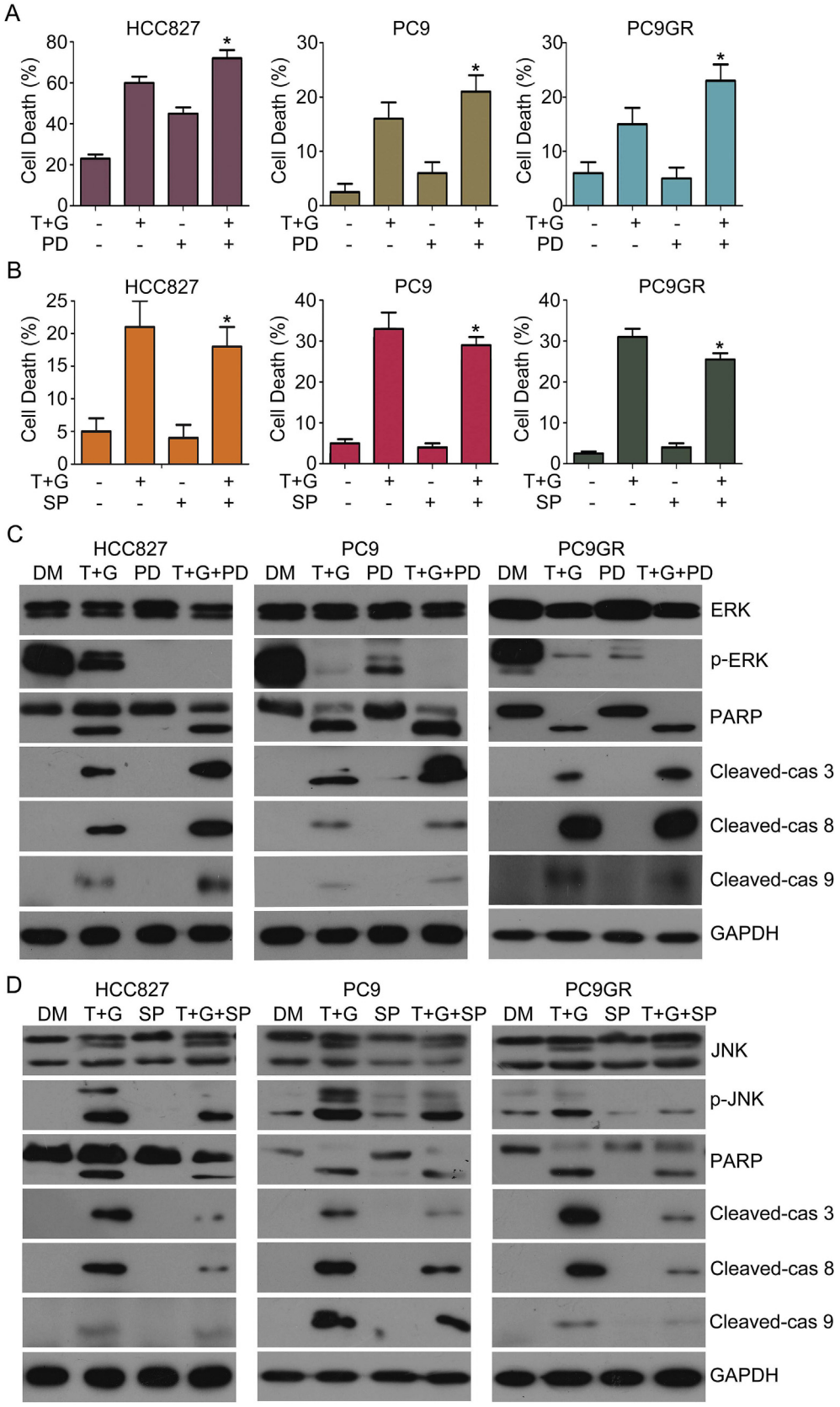

Fig. 5. Inhibition of MEK/ERK and JNK signaling pathways mediate the induction of apoptosis by the co-treatment of thalidomide and gefitinib. HCC827, PC9, and PC9GR cells were treated with thalidomide (75 μM), gefitinib (0.1 μM for HCC827 and PC9, 10 μM for PC9GR), PD0325901 (1 μM)/SP600125 (20 μM), or combination of the three drugs. The collected cells were stained with Annexin V-FITC/PI and subject to flow cytometry to detect cell death. Quantification of cell death is shown (**A** and **B**). *P $<$ 0.05 *vs*. the T + G treatment group. Western blot analysis for the expressions of cleaved caspase −3, −8, −9, and PARP (**C** and **D**).

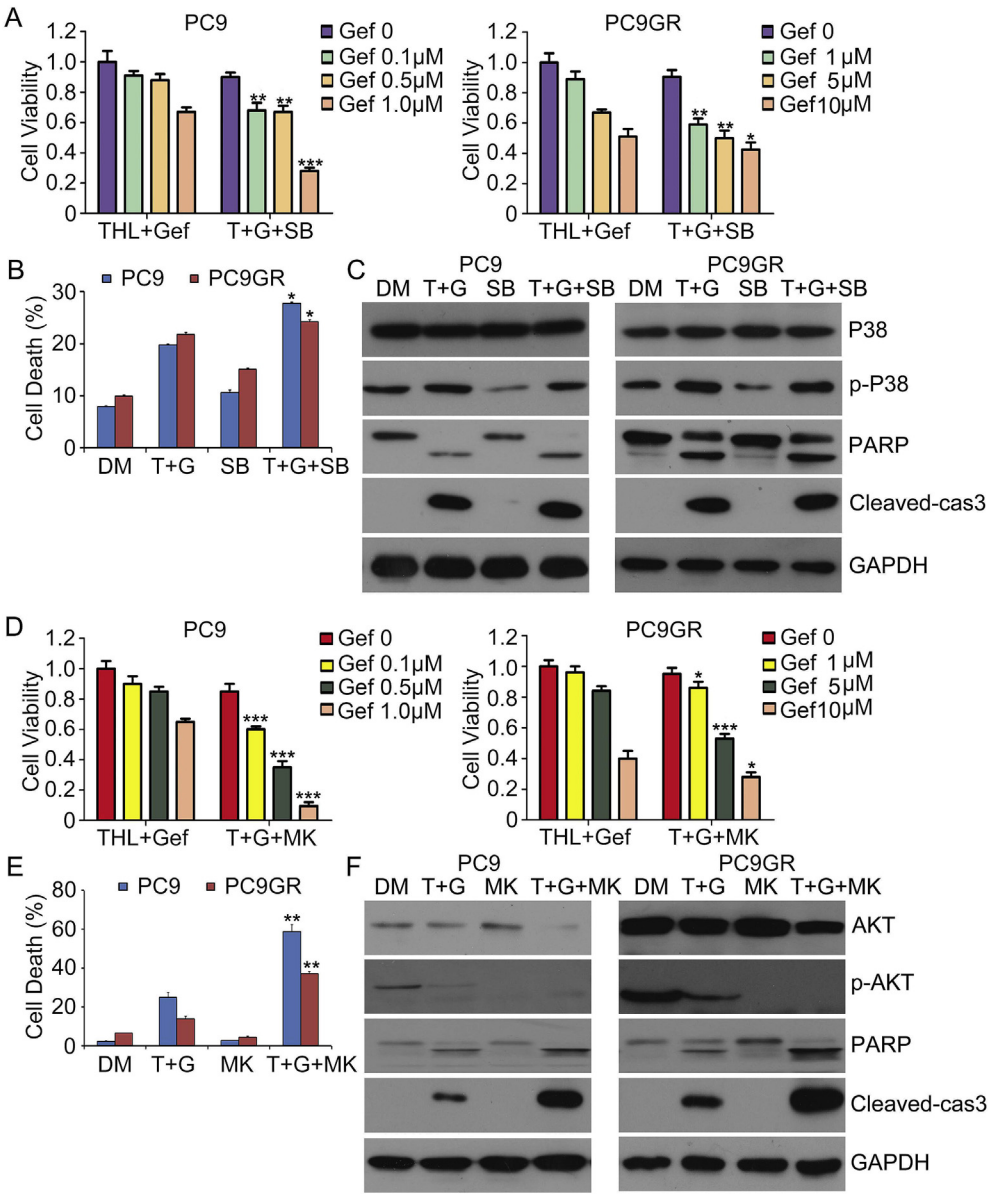

Fig. 6. Inhibition of p38 and PI3K/AKT signaling pathways mediates the induction of apoptosis by the co-treatment of thalidomide and gefitinib. PC9 and PC9GR cells were subjected to the co-treatment of thalidomide (75 μM) and gefitinib (0.1 μM for PC9; 10 μM for PC9GR), SB203580 (10 μM)/MK2206 (5 μM), or the combination of the three drugs for 24 h. (**A** and **D**) MTS assay was used to test the cell viability. The data were derived from three independent experiments. Mean ± S.D. (n = 3). *P < 0.05, **P < 0.01, ***P < 0.001 *vs*. T + G treatment group. The treated cells were stained with Annexin V-FITC/PI. The cell death was analyzed using flow cytometry and the summative data (**B** and **E**) are shown. *P < 0.05, **P < 0.01 *vs*. the T + G treatment group. (**C** and **F**) Western blot analysis for the expression of cleaved caspase −3 and PARP.

second mutation (T790M) on EGFR, nearly 49% of NSCLC patients attained drug resistance, rendering gefitinib ineffective on these patients. Although the second generation of TKIs has been shown to restrain the activation of EGFR with T790M mutation (Arcila et al., 2011), the prolonged usage of the TKIs inevitably gives rise to resistance to the drugs (Walter et al., 2013). Thus, reducing the incidence of drug resistance and overcoming acquired resistance to EGFR-TKI are warranted. In this study, we have demonstrated that a combination of thalidomide with gefitinib show significant synergistic cytostatic and pro-apoptotic effects in NSCLC cells in vitro and in vivo. Notably, the greater antitumor effect of the T + G treatment compared with gefitinib alone seems to be more impressively demonstrated by the in vivo xenograft model than the in vitro cell culture experiments. This phenomenon might be attributable to the following factors. First, the cancer cells in the xenograft experiments had much longer exposure to the treatment regime than they did during the in vitro cell cultures. Conceivably, the longer the treatments last the greater opportunities for the differential benefits to show. Second, T + G might have undergone chemical metabolisms in mice and the resultant metabolites may gain more potent anticancer effects. And lastly, for the transplanted cancer cells to grow into a xenograft tumor and the subsequent growth of the tumor, many processes, such as vascularization and microenvironment establishment, that are not required for cancer cells to grow in the culture dishes must take place. T + G might more effectively affect these processes than gefitinib alone, thereby more appreciably limiting the growth of the xenografts.

Next, we evaluated the effect of the thalidomide and gefitinib combination on cell viability for the first time in NSCLC cell lines, and the co-administration of these drugs showed significant cooperative effects of anti-proliferation in both gefitinib-sensitive and gefitinib-resistant NSCLC cells. Subsequently, we explored whether synergistic growth inhibition of NSCLC cell lines is correlated with cell cycle arrest. Gefitinib remarkably arrests the cell cycle at G0/G1 phase. However, the proportion of cells at the G0/G1 phase did not increase after addition of thalidomide. The levels of CDK4, CDK2, and cyclin D1 were similar between the combined group and the gefitinib alone group; therefore, the antiproliferative effect induced by the combined treatment might not be related to cell cycle inhibition. Despite this phenomenon, higher levels of cell apoptosis were induced by the combined-treatment as indicated by the AnnexinV-FITC/propidium iodide staining data and the increased cleavage of caspase-3, -8, -9, and PARP. Furthermore, the downregulated expressions of Bcl-XL and Bcl-2 and

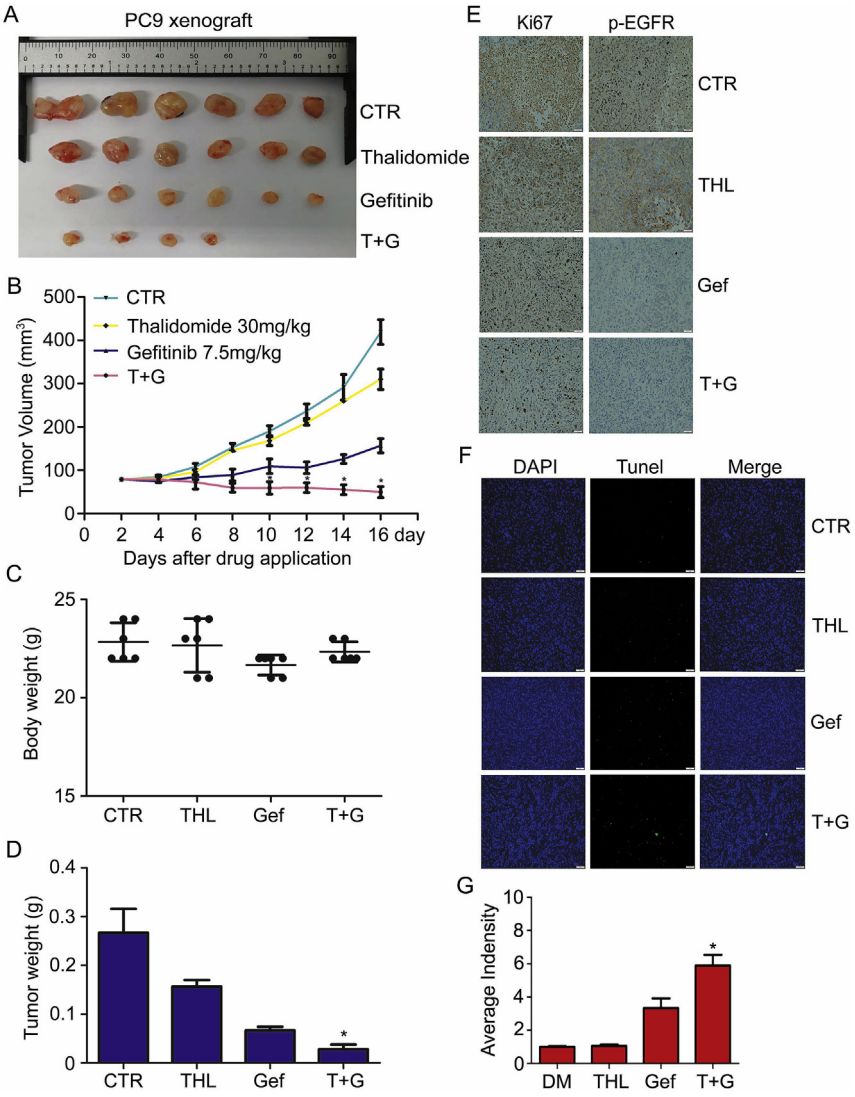

Fig. 7. Co-treatment of thalidomide and gefitinib suppressed the growth of NSCLCs *in vivo*. PC9 cells were injected subcutaneously in BALB/c nude mice treated with thalidomide (30 mg/kg), gefitinib (7.5 mg/kg), or the combination of both for 2 weeks. Tumor sizes (**B**) and the weights of tumor (**D**) and mouse body (**C**) were recorded. Xenograft images (**A**) are shown. *P < 0.05 *vs*. the remaining groups. (**E**) Immunohistochemistry staining for p-EGFR and Ki67 (**E**) and TUNEL staining (**F** and **G**) are shown. *P < 0.05 *vs*. the remaining groups. The represented images were obtained from at least three independent experiments.

the elevated Bax expression were more pronounced after addition of thalidomide. As detected by flow cytometry and Western blot assays, the mitochondrial membrane potential was lower in the combined treatment group than in the single drug treatment groups. In addition, blocking the caspase activation by z-VAD-FMK prevented cell death by the T + G co-treatment. These data suggest that the key cause of the enhanced antiproliferation effect is not cell cycle inhibition but pro-apoptosis.

Gefitinib exerts an inhibitory effect on EGFR phosphorylation (Nguyen and Neal, 2012). PI3K and MAPK signaling pathways are involved in EGFR signal transduction and the AKT phosphorylation is increased in gefitinib-resistant NSCLC cells (Li et al., 2014). Moreover, the inhibition of ERK phosphorylation suppresses the resistance to gefitinib in NSCLC cell lines in vivo and in vitro (Qi et al., 2018). Therefore, we supposed that the marked inhibition of tumor cell proliferation after addition of thalidomide is related to reduction of p-EGFR, p-AKT, and p-ERK. Our results confirmed that thalidomide enhanced the gefitinib-induced reduction of p-EGFR, p-AKT, and p-ERK. Furthermore, the decreased levels of anti-apoptotic p-AKT and p-ERK proteins ascribed the role of diminishing p-AKT and p-ERK to the combined treatment of thalidomide and gefitinib. Consequently, the proportion of cell death induced by the co-treatment of thalidomide and gefitinib was increased when AKT or MEK/ERK was inhibited, suggesting that AKT and MEK/ERK blocked the induction of apoptosis in the combined treatment group. p38 and JNK play critical roles in cell proliferation and survival and are activated by various cellular stresses. In the present study, thalidomide accelerates gefitinib-induced phosphorylation of p38 and JNK. p38 or JNK signaling pathway can be switched off by SB203580 and SP600125, respectively. The JNK inhibitor (SP600125) restrained the apoptosis induced by the combined treatment. Since SP600125 could not completely block the apoptosis induced by the T + G combined treatment, it is very likely that the JNK signaling is not sufficiently robust to counteract the effects of AKT and MEK/ERK in these cancer cells. Hence, JNK is considered responsible for the induction of apoptosis by the T + G combined treatment. However, the inhibition of p38 increased the cell apoptosis induced by the combined treatment rather than suppressing the cell death. Simultaneously, we found that caspase activation was not involved in p38 induced-apoptosis in the combined treatment group; however, the molecular mechanism is yet to be investigated. A previous report showed that blocking p38 MAPK activation by SB202190 enhanced the gefitinib-induced cytotoxicity in human lung cancer cells via inhibition

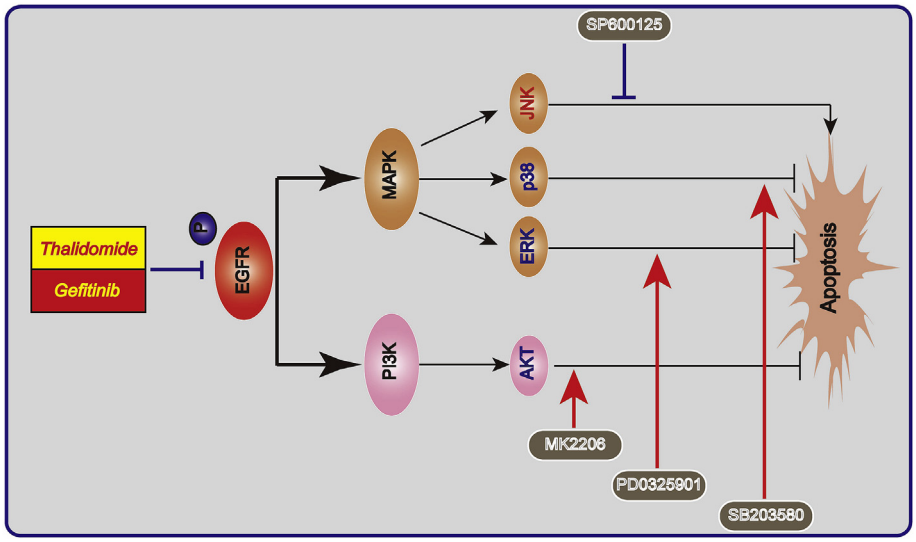

Fig. 8. A proposed model for the inhibition of cell growth by the combination of thalidomide and gefitinib in NSCLC.

of MSH2 (Ko et al., 2013). Thus, we speculated that the cell apoptosis induced by adding p38 inhibitor (SB203580) to the co-treatment of T + G could be similar to that of SB202190(Fig. 8).

The current study has demonstrated that the combination of thalidomide and gefitinib exerts a synergistic cytostatic effect and promises a new therapeutic strategy for lung cancer treatment. Importantly, gefitinib alone and thalidomide alone are frequently used in the clinical treatment of lung cancer and multiple myeloma, respectively (Bringhen et al., 2018; van de Donk et al., 2018). Furthermore, it has been investigated for clinical effect of thalidomide in combination of gefitinib in the treatment of lung cancer (Gu, 2018), suggesting that both drugs are considered safe for the patient and well-tolerated. According to these data, we speculate that NSCLC patients benefit from the combined treatment of thalidomide and gefitinib. By providing these experimental results, we suggest that thalidomide in combination of gefitinib is a promising anti-lung cancer strategy for clinical translation. Nevertheless, future large-scale and prospective clinical trials are essential to investigating the efficacy of gefitinib and thalidomide combined treatment in patients with NSCLCs.

Conflicts of interest

The authors declare no conflict of interest.

Author contribution

H.H., and J.L.: Conceptualization, Data Curation, Funding acquisition, Methodology, Supervision,Writing – Original Draft, Writing-Review & Editing.

X.X., Y.L., YN.,L., Z.G., C.H., F.Z., and L.J.: Conceptualization, Data Curation, Methodology.

X.W.: Writing- Review & Editing.

Acknowledgments

The study was supported by the National Natural Science Foundation of China (81670156, 81872151, 81773213), The National Funds for Developing Local Colleges and Universities (B16056001), Natural Science Foundation research team of Guangdong Province (2018B030312001), the Science and Technology Program of Guangzhou (201604020001), Innovative Academic Team of Guangzhou Education System (1201610014), the Project of Department of Education of Guangdong Province (2016KTSCX119), the Research Team of Department of Education of Guangdong Province (2017KCXTD027), and Guangzhou key medical discipline construction project fund.

We thank Guangdong Provincial Key Laboratory of Malignant Tumor Epigenetics and Gene Regulation, Sun Yat-Sen Memorial Hospital, Sun Yat-Sen University for assistance in flow cytometry analysis.

Appendix A. Supplementary data

Supplementary data to this article can be found online at https://doi.org/10.1016/j.ejphar.2019.172409.

References

Andhavarapu, S., Roy, V., 2013. Immunomodulatory drugs in multiple myeloma. Expert Rev. Hematol. 6, 69–82.
Arcila, M.E., Oxnard, G.R., Nafa, K., Riely, G.J., Solomon, S.B., Zakowski, M.F., Kris, M.G., Pao, W., Miller, V.A., Ladanyi, M., 2011. Rebiopsy of lung cancer patients with acquired resistance to EGFR inhibitors and enhanced detection of the T790M mutation using a locked nucleic acid-based assay. Clin. Cancer Res. 17, 1169–1180.
Bartlett, J.B., Dredge, K., Dalgleish, A.G., 2004. The evolution of thalidomide and its IMiD derivatives as anticancer agents. Nat. Rev. Canc. 4, 314–322.
Bray, F., Ferlay, J., Soerjomataram, I., Siegel, R.L., Torre, L.A., Jemal, A., 2018. Global cancer statistics 2018: GLOBOCAN estimates of incidence and mortality worldwide for 36 cancers in 185 countries. CA A Cancer J. Clin. 68, 394–424.
Bringhen, S., Offidani, M., Palmieri, S., Pisani, F., Rizzi, R., Spada, S., Evangelista, A., Di Renzo, N., Musto, P., Marcatti, M., Vallone, R., Storti, S., Bernardini, A., Centurioni, R., Aitini, E., Palmas, A., Annibali, O., Angelucci, E., Ferrando, P., Baraldi, A., Rocco, S., Andriani, A., Siniscalchi, A., De Stefano, V., Meneghini, V., Palumbo, A., Grammatico, S., Boccadoro, M., Larocca, A., 2018. Early mortality in myeloma patients treated with first-generation novel agents thalidomide, lenalidomide, bortezomib at diagnosis: a pooled analysis. Crit. Rev. Oncol. Hematol. 130, 27–35.
Cai, J., Xia, X., Liao, Y., Liu, N., Guo, Z., Chen, J., Yang, L., Long, H., Yang, Q., Zhang, X., Xiao, L., Wang, X., Huang, H., Liu, J., 2017. A novel deubiquitinase inhibitor b-AP15 triggers apoptosis in both androgen receptor-dependent and -independent prostate cancers. Oncotarget 8, 63232–63246.
Chanan-Khan, A.A., Swaika, A., Paulus, A., Kumar, S.K., Mikhael, J.R., Rajkumar, S.V., Dispenzieri, A., Lacy, M.Q., 2013. Pomalidomide: the new immunomodulatory agent for the treatment of multiple myeloma. Blood Canc. J. 3, e143.
Chen, Z., Fillmore, C.M., Hammerman, P.S., Kim, C.F., Wong, K.K., 2014. Non-small-cell lung cancers: a heterogeneous set of diseases. Nat. Rev. Canc. 14, 535–546.
Chou, T.C., Talalay, P., 1984. Quantitative analysis of dose-effect relationships: the combined effects of multiple drugs or enzyme inhibitors. Adv. Enzym. Regul. 22, 27–55.
Chuah, B., Lim, R., Boyer, M., Ong, A.B., Wong, S.W., Kong, H.L., Millward, M., Clarke, S., Goh, B.C., 2007. Multi-centre phase II trial of Thalidomide in the treatment of unresectable hepatocellular carcinoma. Acta Oncol. 46, 234–238.
Fan, X.X., Li, N., Wu, J.L., Zhou, Y.L., He, J.X., Liu, L., Leung, E.L., 2014. Celastrol induces apoptosis in gefitinib-resistant non-small cell lung cancer cells via caspases-dependent pathways and Hsp90 client protein degradation. Molecules 19, 3508–3522.
Frenzel, A., Grespi, F., Chmelewskij, W., Villunger, A., 2009. Bcl2 family proteins in

carcinogenesis and the treatment of cancer. Apoptosis 14, 584–596.
Gu, J., 2018. Clinical efficacy of gefitinib combined with thalidomide in the treatment of non-small cell lung cancer. China J. Mod. Appl. Pharm. 35, 1073–1074.
Gras, J., 2013. Pomalidomide for patients with multiple myeloma. Drugs Today 49, 555–562.
Huang, H., Chen, D., Li, S., Li, X., Liu, N., Lu, X., Liu, S., Zhao, K., Zhao, C., Guo, H., Yang, C., Zhou, P., Dong, X., Zhang, C., Guanmei Dou, Q.P., Liu, J., 2011. Gambogic acid enhances proteasome inhibitor-induced anticancer activity. Cancer Lett. 301, 221–228.
Huang, H., Guo, M., Liu, N., Zhao, C., Chen, H., Wang, X., Liao, S., Zhou, P., Liao, Y., Chen, X., Lan, X., Chen, J., Xu, D., Li, X., Shi, X., Yu, L., Nie, Y., Wang, X., Zhang, C.E., Liu, J., 2017a. Bilirubin neurotoxicity is associated with proteasome inhibition. Cell Death Dis. 8, e2877.
Huang, H., Liao, Y., Liu, N., Hua, X., Cai, J., Yang, C., Long, H., Zhao, C., Chen, X., Lan, X., Zang, D., Wu, J., Li, X., Shi, X., Wang, X., Liu, J., 2016. Two clinical drugs deubiquitinase inhibitor auranofin and aldehyde dehydrogenase inhibitor disulfiram trigger synergistic anti-tumor effects in vitro and in vivo. Oncotarget 7, 2796–2808.
Huang, H., Liu, N., Liao, Y., Liu, N., Cai, J., Xia, X., Guo, Z., Li, Y., Wen, Q., Yin, Q., Liu, Y., Wu, Q., Rajakumar, D., Sheng, X., Liu, J., 2017b. Platinum-containing compound platinum pyrithione suppresses ovarian tumor proliferation through proteasome inhibition. J. Exp. Clin. Cancer Res. 36, 79.
Huang, H., Zhang, X., Li, S., Liu, N., Lian, W., McDowell, E., Zhou, P., Zhao, C., Guo, H., Zhang, C., Yang, C., Wen, G., Dong, X., Lu, L., Ma, N., Dong, W., Dou, Q.P., Wang, X., Liu, J., 2010. Physiological levels of ATP negatively regulate proteasome function. Cell Res. 20, 1372–1385.
Jones, S., Rappoport, J.Z., 2014. Interdependent epidermal growth factor receptor signalling and trafficking. Int. J. Biochem. Cell Biol. 51, 23–28.
Kirchmair, R., Tietz, A.B., Panagiotou, E., Walter, D.H., Silver, M., Yoon, Y.S., Schratzberger, P., Weber, A., Kusano, K., Weinberg, D.H., Ropper, A.H., Isner, J.M., Losordo, D.W., 2007. Therapeutic angiogenesis inhibits or rescues chemotherapy-induced peripheral neuropathy: taxol- and thalidomide-induced injury of vasa nervorum is ameliorated by VEGF. Mol. Ther. 15, 69–75.
Ko, J.C., Chiu, H.C., Wo, T.Y., Huang, Y.J., Tseng, S.C., Huang, Y.C., Chen, H.J., Syu, J.J., Chen, C.Y., Jian, Y.T., Jian, Y.J., Lin, Y.W., 2013. Inhibition of p38 MAPK-dependent MutS homologue-2 (MSH2) expression by metformin enhances gefitinib-induced cytotoxicity in human squamous lung cancer cells. Lung Cancer 82, 397–406.
Kosaka, T., Yatabe, Y., Endoh, H., Yoshida, K., Hida, T., Tsuboi, M., Tada, H., Kuwano, H., Mitsudomi, T., 2006. Analysis of epidermal growth factor receptor gene mutation in patients with non-small cell lung cancer and acquired resistance to gefitinib. Clin. Cancer Res. 12, 5764–5769.
Kumar, S., Rajkumar, S.V., 2005. Thalidomide and dexamethasone: therapy for multiple myeloma. Expert Rev. Anticancer Ther. 5, 759–766.
Kumar, S., Witzig, T.E., Rajkumar, S.V., 2002. Thalidomide as an anti-cancer agent. J. Cell Mol. Med. 6, 160–174.
Lenardo, T.M., Calabrese, L.H., 2000. The role of thalidomide in the treatment of rheumatic disease. J. Clin. Rheumatol. 6, 19–26.
Li, L., Han, R., Xiao, H., Lin, C., Wang, Y., Liu, H., Li, K., Chen, H., Sun, F., Yang, Z., Jiang, J., He, Y., 2014. Metformin sensitizes EGFR-TKI-resistant human lung cancer cells in vitro and in vivo through inhibition of IL-6 signaling and EMT reversal. Clin. Cancer Res. 20, 2714–2726.
Liao, Y., Liu, N., Hua, X., Cai, J., Xia, X., Wang, X., Huang, H., Liu, J., 2017. Proteasome-associated deubiquitinase ubiquitin-specific protease 14 regulates prostate cancer proliferation by deubiquitinating and stabilizing androgen receptor. Cell Death Dis. 8, e2585.
Liao, Y., Xia, X., Liu, N., Cai, J., Guo, Z., Li, Y., Jiang, L., Dou, Q.P., Tang, D., Huang, H., Liu, J., 2018. Growth arrest and apoptosis induction in androgen receptor-positive human breast cancer cells by inhibition of USP14-mediated androgen receptor deubiquitination. Oncogene 37, 1896–1910.
Lin, Y.C., Shun, C.T., Wu, M.S., Chen, C.C., 2006. A novel anticancer effect of thalidomide: inhibition of intercellular adhesion molecule-1-mediated cell invasion and metastasis through suppression of nuclear factor-kappaB. Clin. Cancer Res. 12, 7165–7173.
Loong, H.H., Kwan, S.S., Mok, T.S., Lau, Y.M., 2018. Therapeutic strategies in EGFR mutant non-small cell lung cancer. Curr. Treat. Options Oncol. 19, 58.
Lu, P.H., Kuo, T.C., Chang, K.C., Chang, C.H., Chu, C.Y., 2011. Gefitinib-induced epidermal growth factor receptor-independent keratinocyte apoptosis is mediated by the JNK activation pathway. Br. J. Dermatol. 164, 38–46.
Matarrese, P., Falzano, L., Fabbri, A., Gambardella, L., Frank, C., Geny, B., Popoff, M.R., Malorni, W., Fiorentini, C., 2007. Clostridium difficile toxin B causes apoptosis in epithelial cells by thrilling mitochondria. Involvement of ATP-sensitive mitochondrial potassium channels. J. Biol. Chem. 282, 9029–9041.
McMeekin, D.S., Sill, M.W., Darcy, K.M., Stearns-Kurosawa, D.J., Webster, K., Waggoner, S., Benbrook, D., 2007. A phase II trial of thalidomide in patients with refractory leiomyosarcoma of the uterus and correlation with biomarkers of angiogenesis: a gynecologic oncology group study. Gynecol. Oncol. 106, 596–603.
Mitsudomi, T., Yatabe, Y., 2010. Epidermal growth factor receptor in relation to tumor development: EGFR gene and cancer. FEBS J. 277, 301–308.
Nguyen, K.S., Neal, J.W., 2012. First-line treatment of EGFR-mutant non-small-cell lung cancer: the role of erlotinib and other tyrosine kinase inhibitors. Biologics 6, 337–345.
Pao, W., Miller, V.A., Politi, K.A., Riely, G.J., Somwar, R., Zakowski, M.F., Kris, M.G., Varmus, H., 2005. Acquired resistance of lung adenocarcinomas to gefitinib or erlotinib is associated with a second mutation in the EGFR kinase domain. PLoS Med. 2, e73.
Pinter, M., Wichlas, M., Schmid, K., Plank, C., Muller, C., Wrba, F., Peck-Radosavljevic, M., 2008. Thalidomide in advanced hepatocellular carcinoma as antiangiogenic treatment approach: a phase I/II trial. Eur. J. Gastroenterol. Hepatol. 20, 1012–1019.
Qi, M., Tian, Y., Li, W., Li, D., Zhao, T., Yang, Y., Li, Q., Chen, S., Yang, Y., Zhang, Z., Tang, L., Liu, Z., Su, B., Li, F., Feng, Y., Fei, K., Zhang, P., Zhang, F., Zhang, L., 2018. ERK inhibition represses gefitinib resistance in non-small cell lung cancer cells. Oncotarget 9, 12020–12034.
Qiao, Z., Yuan, J., Shen, J., Wang, C., He, Z., Hu, Y., Zhang, M., Xu, C., 2015. Effect of thalidomide in combination with gemcitabine on human pancreatic carcinoma SW-1990 cell lines in vitro and in vivo. Oncol Lett. 9, 2353–2360.
Rajkumar, S.V., Hayman, S., Gertz, M.A., Dispenzieri, A., Lacy, M.Q., Greipp, P.R., Geyer, S., Iturria, N., Fonseca, R., Lust, J.A., Kyle, R.A., Witzig, T.E., 2002. Combination therapy with thalidomide plus dexamethasone for newly diagnosed myeloma. J. Clin. Oncol. 20, 4319–4323.
Raymond, E., Faivre, S., Armand, J.P., 2000. Epidermal growth factor receptor tyrosine kinase as a target for anticancer therapy. Drugs 60 (Suppl. 1), 15–23 discussion 41-12.
Roberts, P.J., Der, C.J., 2007. Targeting the Raf-MEK-ERK mitogen-activated protein kinase cascade for the treatment of cancer. Oncogene 26, 3291–3310.
Sequist, L.V., Waltman, B.A., Dias-Santagata, D., Digumarthy, S., Turke, A.B., Fidias, P., Bergethon, K., Shaw, A.T., Gettinger, S., Cosper, A.K., Akhavanfard, S., Heist, R.S., Temel, J., Christensen, J.G., Wain, J.C., Lynch, T.J., Vernovsky, K., Mark, E.J., Lanuti, M., Iafrate, A.J., Mino-Kenudson, M., Engelman, J.A., 2011. Genotypic and histological evolution of lung cancers acquiring resistance to EGFR inhibitors. Sci. Transl. Med. 3 75ra26.
Shih, J.Y., Gow, C.H., Yang, P.C., 2005. EGFR mutation conferring primary resistance to gefitinib in non-small-cell lung cancer. N. Engl. J. Med. 353, 207–208.
Silvestri, G.A., Spiro, S.G., 2006. Carcinoma of the bronchus 60 years later. Thorax 61, 1023–1028.
Son, M.J., Kim, J.S., Kim, M.H., Song, H.S., Kim, J.T., Kim, H., Shin, T., Jeon, H.J., Lee, D.S., Park, S.Y., Kim, Y.J., Kim, J.H., Nam, D.H., 2006. Combination treatment with temozolomide and thalidomide inhibits tumor growth and angiogenesis in an orthotopic glioma model. Int. J. Oncol. 28, 53–59.
Soria, J.C., Mok, T.S., Cappuzzo, F., Janne, P.A., 2012. EGFR-mutated oncogene-addicted non-small cell lung cancer: current trends and future prospects. Cancer Treat Rev. 38, 416–430.
Stein, E.M., Rivera, C., 2007. Transient thyroiditis after treatment with lenalidomide in a patient with metastatic renal cell carcinoma. Thyroid 17, 681–683.
van de Donk, N.W., van der Holt, B., Minnema, M.C., Vellenga, E., Croockewit, S., Kersten, M.J., von dem Borne, P.A., Ypma, P., Schaafsma, R., de Weerdt, O., Klein, S.K., Delforge, M., Levin, M.D., Bos, G.M., Jie, K.G., Sinnige, H., Coenen, J.L., de Waal, E.G., Zweegman, S., Sonneveld, P., Lokhorst, H.M., 2018. Thalidomide before and after autologous stem cell transplantation in recently diagnosed multiple myeloma (HOVON-50): long-term results from the phase 3, randomised controlled trial. Lancet Haematol. 5, e479–e492.
Walter, A.O., Sjin, R.T., Haringsma, H.J., Ohashi, K., Sun, J., Lee, K., Dubrovskiy, A., Labenski, M., Zhu, Z., Wang, Z., Sheets, M., St Martin, T., Karp, R., van Kalken, D., Chaturvedi, P., Niu, D., Nacht, M., Petter, R.C., Westlin, W., Lin, K., Jaw-Tsai, S., Raponi, M., Van Dyke, T., Etter, J., Weaver, Z., Pao, W., Singh, J., Simmons, A.D., Harding, T.C., Allen, A., 2013. Discovery of a mutant-selective covalent inhibitor of EGFR that overcomes T790M-mediated resistance in NSCLC. Cancer Discov. 3, 1404–1415.
Wang, J., Li, X., Xue, X., Ou, Q., Wu, X., Liang, Y., Wang, X., You, M., Shao, Y.W., Zhang, Z., Zhang, S., 2018. Clinical outcomes of EGFR kinase domain duplication to targeted therapies in NSCLC. Int. J. Cancer 144, 2677–2682.
Woo, K., Stewart, S.G., Kong, G.S., Finch-Edmondson, M.L., Dwyer, B.J., Yeung, S.Y., Abraham, L.J., Kampmann, S.S., Diepeveen, L.A., Passman, A.M., Elsegood, C.L., Tirnitz-Parker, J.E., Callus, B.A., Olynyk, J.K., Yeoh, G.C., 2016. Identification of a thalidomide derivative that selectively targets tumorigenic liver progenitor cells and comparing its effects with lenalidomide and sorafenib. Eur. J. Med. Chem. 120, 275–283.
Xia, X., Liao, Y., Guo, Z., Li, Y., Jiang, L., Zhang, F., Huang, C., Liu, Y., Wang, X., Liu, N., Liu, J., Huang, H., 2018. Targeting proteasome-associated deubiquitinases as a novel strategy for the treatment of estrogen receptor-positive breast cancer. Oncogenesis 7, 75.
Yochum, Z.A., Cades, J., Wang, H., Chatterjee, S., Simons, B.W., O'Brien, J.P., Khetarpal, S.K., Lemtiri-Chlieh, G., Myers, K.V., Huang, E.H., Rudin, C.M., Tran, P.T., Burns, T.F., 2019. Targeting the EMT transcription factor TWIST1 overcomes resistance to EGFR inhibitors in EGFR-mutant non-small-cell lung cancer. Oncogene 38, 656–670.
Yu, H.A., Arcila, M.E., Rekhtman, N., Sima, C.S., Zakowski, M.F., Pao, W., Kris, M.G., Miller, V.A., Ladanyi, M., Riely, G.J., 2013. Analysis of tumor specimens at the time of acquired resistance to EGFR-TKI therapy in 155 patients with EGFR-mutant lung cancers. Clin. Cancer Res. 19, 2240–2247.